Synthesis and Characterization of Crystalline Ag_2Se Nanowires Through a Template-Engaged Reaction at Room Temperature**

By *Byron Gates*, *Brian Mayers*, *Yiying Wu*, *Yugang Sun*, *Bryan Cattle*, *Peidong Yang*, and *Younan Xia**

Single-crystalline Ag_2Se nanowires have been successfully synthesized through a template-engaged topotactic reaction in which nanowires of trigonal selenium were transformed into Ag_2Se by reacting with aqueous $AgNO_3$ solutions at room temperature (RT). An interesting size-dependent transition between two crystal structures has also been observed for this newly synthesized one-dimensional system: The Ag_2Se nanowires adopted a tetragonal structure when their diameters were less than ~40 nm; an orthorhombic structure was found to be more favorable as the diameter of these nanowires was increased beyond 40 nm. Since this reaction can be carried out at ambient pressure and temperature, it should be straightforward to scale up the entire process for the high-volume production of Ag_2Se nanowires with well-controlled sizes and crystal structures. These highly uniform nanowires of single-crystalline Ag_2Se are potentially useful as photosensitizers, superionic conductors, magnetoresistive compounds, or thermoelectric materials. This work also represents the first demonstration of a template-engaged process capable of generating single-crystalline nanowires from the solution-phase and at RT.

1. Introduction

One-dimensional (1D) nanostructures (such as wires, rods, and tubes) have been the subject of intensive research due to their niche application in fabricating nanoscale electronic, photonic, electrochemical, and electromechanical devices.[1] Nanowires, in particular, have been recognized as the necessary functional components and interconnects in building nanocircuitry through self-assembly.[2] Nanowires with uniform diameters also represent an ideal system for investigating the dependence of transport and mechanical properties on size confinement.[3] As an alternative route complementary to advanced nanolithographic techniques, a number of chemical methods (or the so-called bottom-up approach) have recently been demonstrated or reexamined for generating 1D nanostructures.[4] These methods offer a range of advantages over the lithographic techniques in terms of cost, versatility, and the potential for high-volume production. Among these chemical methods, the most successful examples seem to be those based on vapor–solid (VS), vapor–liquid–solid (VLS), solution–liquid–solid (SLS), and solution–solid (SS) processes. 1D nanostructures that have been produced through these methods include carbon nanotubes and their derivatives,[5] nanowires of metals and semiconductors,[6] and nanowhiskers (or nanorods) of various inorganic substances.[7] These chemical methods may require the use of exotic, dual-functional nanocrystallites capable of serving as both catalysts, and seeds for the anisotropic growth of nanostructures characterized by 1D morphologies. The difficulty in selecting a suitable catalyst has greatly limited the scope of materials that could be processed into nanowires (or rods) using these procedures.

Template-directed synthesis represents another straightforward strategy for generating 1D nanostructures. In this approach, the templates may serve as physical scaffolds against which other materials are assembled or processed into nanostructures with a morphology similar (or complementary) to that of the original template. A rich variety of 1D templates have been successfully demonstrated for use with this approach, with notable examples including channels in porous materials,[8] hexagonal assemblies of surfactants or organic block copolymers,[9] and 1D nanostructures synthesized using other chemical methods.[10] In some cases, the templates are actively engaged in the synthesis as one of the reactants. Such cases are called template-engaged reactions. For example, Lieber et al. demonstrated that carbon nanotubes could react with metal oxides at elevated temperatures to form whiskers of various functional materials such as SiC.[11] Fan et al. further explored this idea and demonstrated that carbon nanotubes could be used as sacrificial templates to generate nanorods of III–V compounds.[12] Because the templates were consumed during these chemical templating processes, the pure product could be easily obtained without additional post-treatments such as dissolution or removal of the templates.

Although the capability and versatility of both physical and chemical templating processes have been demonstrated for a range of materials, they often generate polycrystalline nano-

[*] Prof. Y. Xia, Dr. B. Gates, B. Mayers, Dr. Y. Sun, B. Cattle
Department of Chemistry, University of Washington
Seattle, WA 98195-1700 (USA)
E-mail: xia@chem.washington.edu
Y. Wu, Prof. P. Yang
Department of Chemistry, University of California
Berkeley, CA 94720 (USA)

[**] This work has been supported in part by a Fellowship from the David and Lucile Packard Foundation (UW), Career Awards from the National Science Foundation (DMR-9983893 at UW; DMR-0092086 at UCB), Research Fellowships from the Alfred P. Sloan Foundation (UW and UCB); and New Faculty Awards from the Dreyfus Foundation (UW and UCB). B. Gates and B. Mayers thank the Center for Nanotechnology at the UW for two IGERT Fellowships supported by the National Science Foundation (DGE-9987620).

  1616-301X/02/1010-0679 $ 17.50+.50/0

wires that can be limited in use for property measurements and device fabrication. In addition, although those nanowires formed via reactions with carbon nanotubes were characterized by highly crystalline structures, these reactions needed to be carried out at relatively high temperatures (e.g., 800–1200 °C). Here, we would like to present the detailed study of a template-engaged reaction, by which single-crystalline nanowires of trigonal selenium could be quantitatively converted into single-crystalline nanowires of Ag_2Se by reacting with aqueous solutions of silver nitrate at ambient temperature and pressure.[13] In this process, both morphology and dimensions of the original template could be retained in the final product with high fidelity.

Silver selenide has been extensively studied in literature due to its many interesting and useful properties.[14] Its high-temperature phase (β-Ag_2Se, > 133 °C) is a superionic conductor that has been utilized as the solid electrolyte in photochargable secondary batteries. The low-temperature phase (α-Ag_2Se, < 133 °C) is a narrow bandgap semiconductor with an energy gap of ~0.07 eV near 0 K. It has been widely exploited for use as a thermochromic material, as well as a photosensitizer in photographic processing. The low-temperature phase of silver selenide is also a promising candidate for thermoelectric applications because of its relatively high Seebeck coefficient (–150 $\mu V K^{-1}$ at 300 K), low thermal conductivity, and high electrical conductivity.[15] More recently, large magnetoresistance was also reported for a non-stoichiometric derivative of this solid.[16] It is reasonable to argue that the availability of high quality Ag_2Se nanowires could spawn new applications, and/or significantly enhance the performance of many currently existing devices as a result of their one-dimensionality and quantum confinement effects.

Conventional syntheses of silver selenide include vapor phase growth, high temperature and high pressure solution-phase reactions, and sonochemical routes. It has been demonstrated that Ag_2Se forms spontaneously at the interface when a polycrystalline film of silver was deposited onto amorphous selenium in the vapor phase.[17] Recently, Qian et al. reported a hydrothermal approach to Ag_2Se nanocrystals that used silver nitrate and elemental selenium as precursors.[18] Similar products were also obtained when silver ions reacted with elemental selenium in non-aqueous solvents. For example, Xie et al. has demonstrated a procedure for synthesizing Ag_2Se nanocrystals in pyridine via the reaction of $AgNO_3$ and Se with KBH_4, or in ethylenediamine through sonochemical activation.[19] Silver selenide has also been directly synthesized from elemental precursors through high-pressure reactions in liquid ammonia carried out at RT.[20] All these routes to Ag_2Se, however, did not provide a good control over size and morphology for the resultant nanostructures. The final products were typically polydispersed colloidal (zero-dimensional) or whiskers with low aspect ratios. Most of these procedures also required relatively high temperatures and/or pressures. The synthetic route to Ag_2Se nanowires described in the present paper is advantageous because it proceeds at room temperature (RT) and in aqueous media. The morphology and size of the Ag_2Se nanowires could be precisely controlled because the reaction was tightly confined by the single-crystalline template made of trigonal selenium. Silver selenide nanowires obtained using this procedure were also uniform in diameter, single-crystalline in structure, and displayed aspect ratios as high as 1000.

2. Results and Discussion

The present synthesis of silver selenide nanowires followed the procedure briefly described in a previous communication.[13] The first step of this process involved the synthesis of single-crystalline selenium nanowires in the aqueous phase via a solid-solution-solid transformation of amorphous selenium (*a*-Se) colloids into trigonal selenium (*t*-Se) nanowires.[21] Nanowires of Ag_2Se were synthesized through a solid-solution reaction that used the single-crystalline *t*-Se nanowires as chemical templates. Although the transformation of nanostructures into different materials with the similar morphology is not a new concept,[11,12] the template-engaged reaction described in this article differs from previous methods by its utilization of a RT, topotactic reaction, through which the morphology and single-crystallinity of the nanowire templates could be retained with high fidelity.

2.1. Characterization of *t*-Se Nanowires

The templates—uniform nanowires of *t*-Se—were synthesized using a procedure reported previously,[21] which involved the reduction of selenious acid precursor with hydrazine to form colloidal particles of *a*-Se at elevated temperatures:

$$H_2SeO_{3(aq)} + N_2H_{4(aq)} \rightarrow Se_{(s)} + 3H_2O + N_{2(g)} \quad (1)$$

As the reaction mixture was cooled down, crystalline seeds of *t*-Se were generated in the solution through a homogeneous nucleation process. These *t*-Se seeds grew into high aspect ratio nanowires over time as the less stable *a*-Se colloids were slowly dissolved into solution. In this solid-solution-solid transformation, the 1D morphology of the final product was solely determined by the highly anisotropic characteristics of the building blocks—that is, the linearity of infinite, helical chains of selenium atoms contained in the trigonal phase. The diameter of these *t*-Se nanowires was defined by the lateral dimensions of the nanocrystalline seeds. Using this process, uniform single-crystalline nanowires with diameters ranging from 10 nm to 800 nm could be synthesized.

Figures 1A and B show scanning electron microscopy (SEM) and transmission electron microscopy (TEM) images of single-crystalline *t*-Se nanowires with a mean diameter of 32 nm. These images indicate the copiousness in quantity, the uniformity in lateral dimensions, and the uniformity along the longitudinal axis that could be routinely achieved for these 1D nanostructures. The inset of Figure 1B displays an electron microdiffraction pattern that was obtained from an individual nanowire. This diffraction pattern suggests that the nanowires

  1616-301X/02/1010-0680 $ 17.50+.50/0

ADVANCED FUNCTIONAL MATERIALS

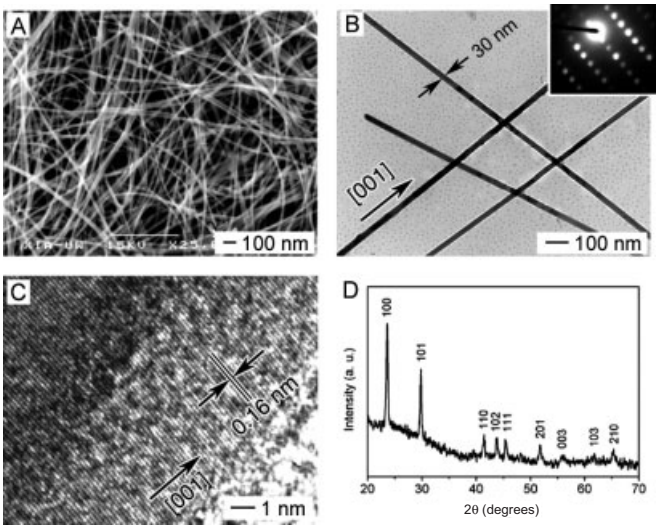

Fig. 1. A) SEM image of *t*-Se nanowires with a mean diameter of 32 ± 5 nm grown from an aqueous reaction mixture refluxed at 100 °C. B) TEM image of several such *t*-Se nanowires prepared from the same reaction solution as in (A), after diluting by ~20 times. The inset gives a typical electron microdiffraction pattern that was obtained by focusing the beam on an individual nanowire. This pattern confirms that the selenium was crystallized in the trigonal phase, with the helical chains of selenium atoms packed parallel to each other and along the longitudinal axis of each nanowire. C) HRTEM image taken from one such nanowire further conferring their single-crystalline structure. The fringe spacing (~0.16 nm) observed in this image corresponds to the separation between the (003) lattice planes. D) An XRD pattern of these nanowires supported on a glass slide. All peaks could be indexed to the trigonal phase of Se.

synthesized using this procedure were single-crystalline, and that they predominantly grew along the <001> direction, or the *c*-axis of the trigonal phase. The lattice constants ($a = 0.436$ nm and $c = 0.495$ nm) calculated from this diffraction pattern are also consistent with those of *t*-Se, with infinite spiral chains of selenium atoms parallel to the *c*-axis.[22] The single-crystalline nature and structural parameters of these wires were further confirmed by the high-resolution TEM image shown in Figure 1C. The fringe spacing (~0.16 nm) calculated from this image corresponds to the separation between the (003) lattice planes. Figure 1D shows a typical XRD pattern for 32 nm diameter nanowires of *t*-Se. All the diffraction peaks could be indexed as the trigonal phase of selenium. The abnormal intensity of the (100) peak (as compared to that of polycrystalline samples) indicated that these selenium nanowires had been preferentially grown along the *c*-axis, the <001> direction. The results of the XRD measurements, performed on samples containing relatively large quantities of nanowires, indicate the high purity of *t*-Se nanowires produced using the present chemical approach. The single-crystallinity and absence of kinks or other related defects within these nanowires should make them particularly useful as solid templates in generating nanowires made of other functional materials.

2.2. Transformation of *t*-Se into Ag_2Se Nanowires

Silver selenide nanowires could be formed through a template-engaged reaction between *t*-Se nanowires and Ag^+ ions (added in the form of aqueous $AgNO_3$). The net reaction involved in this process can be summarized as the following:

$$3Se_{(s)} + 6Ag^+_{(aq)} + 3H_2O \rightarrow 2Ag_2Se_{3(s)} + Ag_2SeO_{3(s)} + 6H^+_{(aq)} \quad (2)$$

The changes in crystallinity, completion of reaction, and purity (composition and phase) of this synthesis were studied by XRD measurements. In a typical procedure, the *t*-Se nanowires could be fully converted into the products within a period of ~2 h, depending on the molar ratio between reagents. The solid templates (*t*-Se nanowires) could be either maintained as aqueous suspensions or supported on TEM grids, and all reactions were carried out at RT. In addition to the desired silver selenide product, a solid byproduct (Ag_2SeO_3) was also formed. This byproduct could be readily removed (to isolate the pure Ag_2Se nanowires) by rinsing the reaction mixture with excess hot water (~90 °C).

Powder X-ray diffraction provides a convenient means to follow the progression of this reaction as a function of time and the molar ratio between reagents. Figure 2 shows the time dependence of this process that was determined for *t*-Se nanowires of ~800 nm in diameter, with the molar ratio between Se and Ag^+ being 1:50 for each reaction. In this study, the reaction was quenched at the set-time by removing the solvent through filtration. The solid mixture was then rinsed with hot water (~90 °C) to remove monoclinic Ag_2SeO_3 solid prior to acquiring the XRD patterns. The topmost trace of this figure shows the XRD pattern of pure *t*-Se nanowires (~800 nm in diameter) prior to reaction with silver nitrate solution. All of the peaks that were present could be indexed to the trigonal phase of selenium. The other patterns shown in this figure suggest a continuous transformation of selenium nanowire templates into silver selenide. After a period of ~2 h, all peaks associated with

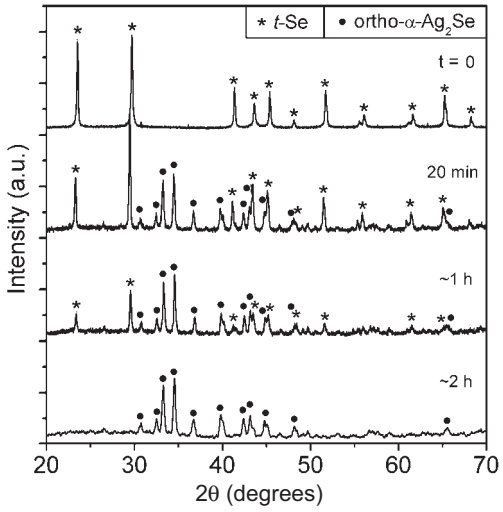

Fig. 2. XRD patterns (offset for clarity) of ~800 nm selenium nanowires after reacting with aqueous solutions of silver nitrate for the designated lengths of time. Single-crystalline nanowires of *t*-Se were completely converted to silver selenide within 2 h at room temperature. All samples were rinsed with hot water (~90 °C) to remove Ag_2SeO_3 prior to analysis.

  1616-301X/02/1010-0681 $ 17.50+.50/0

t-Se had disappeared indicating complete transformation of the starting material into orthorhombic silver selenide. For selenium nanowires with smaller diameters, the reaction should be completed within short periods of time.

Figure 3 shows the XRD patterns of reaction products where the molar ratio between Se and Ag^+ was increased from 1:4 to 1:9 and 1:50. The reagents were brought into contact and allowed to react for ~12 h before the reaction was quenched (by filtration) for XRD analysis. When *t*-Se nanowires were reacted with silver nitrate at a mole ratio of 1:4, the appearance of new peaks after 12 h of reaction confirmed the formation of orthorhombic silver selenide. As the relative concentration of silver ions was increased from 1:4 to 1:9 and 1:50, the intensity of the characteristic *t*-Se diffraction peaks decreased and eventually disappeared. The byproduct of this reaction—monoclinic silver selenite (Ag_2SeO_3)—was also observed along with orthorhombic silver selenide in all XRD patterns. As noted above, this byproduct could be selectively removed by rinsing the samples with excess hot water.

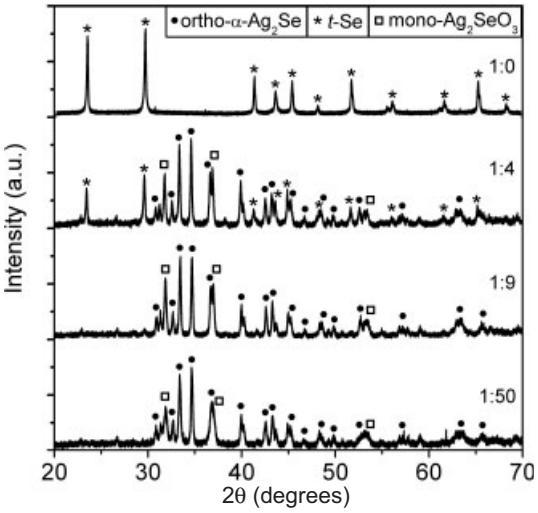

Fig. 3. XRD patterns of the as-synthesized products after reacting trigonal selenium wires (~800 nm in diameter) with silver nitrate solutions of increasing concentrations. Conversion of *t*-Se to orthorhombic α-Ag_2Se was only completed at high concentrations of silver nitrate (e.g., with a molar ratio of selenium to silver > 1:50). These XRD patterns also indicate the formation of a mixture of orthorhombic α-Ag_2Se and monoclinic Ag_2SeO_3 solids. The Ag_2SeO_3 solid could be selectively removed from the mixture by rinsing with hot water (~90 °C).

2.3. Structural Characterization of Ag_2Se Nanowires

The chemical transformation of *t*-Se into Ag_2Se (as indicated by XRD measurements) was further supported by electron microscopy and diffraction studies, which also indicated that the transformation of *t*-Se into Ag_2Se nanowires closely maintained the morphology and dimensions of the initial templates. In Figure 4A, for example, *t*-Se templates of ~100 nm in diameter were fully converted into orthorhombic Ag_2Se with high fidelity. The EDX pattern shown in Figure 4B also indicated that the template had been completely transformed into a product with a Ag/Se elemental ratio of approximately 2. The water-soluble byproduct, monoclinic Ag_2SeO_3, had been removed from this sample before taking the EDX spectrum. Figure 4C shows the TEM image and microdiffraction pattern (inset) of an individual as-synthesized 50 nm Ag_2Se nanowire. The twofold, rotational symmetry associated with this pattern suggests that the longitudinal axis of this Ag_2Se nanowire was predominantly along the <100> direction.[23] This diffraction pattern also indicates that this Ag_2Se nanowire was crystallized in the orthorhombic phase. The lattice constants calculated from this diffraction pattern ($a = 0.705$ nm, $b = 0.782$ nm, and $c = 0.434$ nm) matched very well with those of the orthorhombic silver selenide ($a = 0.706$ nm, $b = 0.776$ nm, and $c = 0.433$ nm) reported in literature.[24] Diffraction patterns taken from different regions of this individual nanowire were essentially the same. Such homogeneity in crystalline structure and orientation along each nanowire implies that the Ag_2Se nanowires synthesized using the present procedure were single-crystalline in structure. This conclusion was supported by HRTEM studies (Figs. 4D). The fringe spacing observed in this image matched well with the separation between the (200) planes of orthorhombic silver selenide. HRTEM analysis across an individual nanowire further confirms the absence of domain boundaries within each individual nanowire.

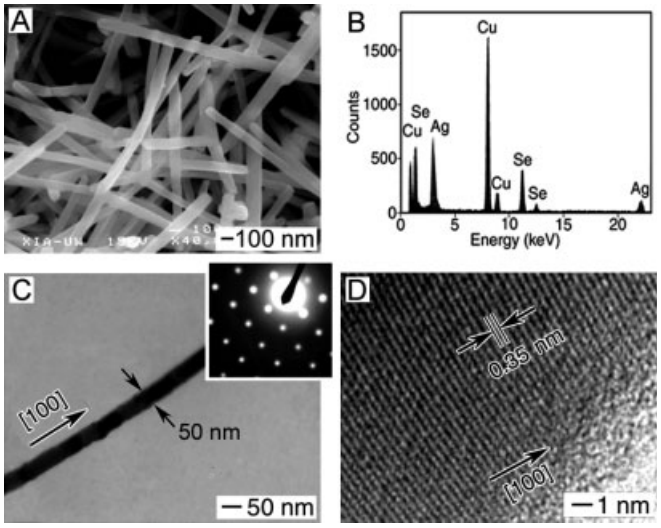

Fig. 4. A) SEM image of α-Ag_2Se nanowires synthesized by reacting ~100 nm nanowires of *t*-Se with an aqueous silver nitrate solution. B) The EDX spectrum of these α-Ag_2Se nanowires, indicating the stoichiometry of the products. The ratio of silver to selenium was found to be 2:1 as expected for silver selenide. The presence of copper was due to the fact that the sample was mounted on a copper TEM grid. C) The TEM image and microdiffraction pattern (inset) of an α-Ag_2Se nanowire whose diameter was ~50 nm. The diffraction spots could be indexed to the orthorhombic structure; this assignment is further supported by the HRTEM image shown in (D). The longitudinal axis of such nanowires of orthorhombic Ag_2Se were along the <100> direction. The fringe spacing (~0.35 nm) observed in this image corresponds to the separation between the (200) lattice planes.

2.4. Size Dependence for the Structure of Ag_2Se Nanowires

During our microscopic analysis, we also found a diameter-dependent transformation for the structures of these single-crystalline nanowires Ag_2Se. As shown in the previous section,

  1616-301X/02/1010-0682 $ 17.50+.50/0 *Adv. Funct. Mater.* **2002**, *12*, No. 10, October

ADVANCED FUNCTIONAL MATERIALS

selenium nanowires with diameters > 40 nm were quantitatively converted to Ag_2Se nanowires with an orthorhombic structure. When selenium templates with diameters < 40 nm were used, however, the tetragonal structure was found to be more favorable. Figure 5 shows the SEM and TEM images of α-Ag_2Se nanowires that were generated by reacting with the

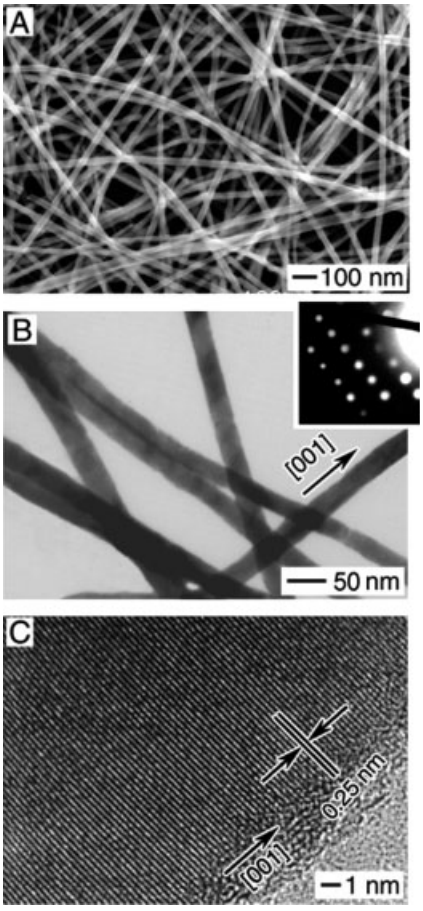

Fig. 5. The SEM (A) and TEM (B) images of uniform nanowires of α-Ag_2Se synthesized through a reaction between 32 nm nanowires of *t*-Se and an aqueous solution of silver nitrate at room temperature. The inset in (B) gives a typical microdiffraction pattern that was obtained by focusing the electron beam on an individual wire. These low-temperature Ag_2Se nanowires had a tetragonal structure, and the longitudinal axis of each wire was along the <001> direction. The single-crystallinity of these wires was further confirmed by the HRTEM image shown in (C). The fringe spacing of ~0.25 nm corresponds to the separation between the (002) lattice planes.

32 nm nanowires of *t*-Se shown in Figure 1. It can be seen again that the dimensions and morphology of the initial *t*-Se templates were retained with high fidelity during this solid-solution reaction. The as-synthesized nanowires of Ag_2Se were analyzed for purity of phase and composition using several techniques. The XRD pattern indicated that these Ag_2Se nanowires were crystallized in the tetragonal phase with lattice constants $a = b = 0.698$ nm, and $c = 0.496$ nm. The EDX analysis confirmed that these nanowires consisted of the expected 1:2 stoichiometric ratio for selenium and silver. The smooth surfaces and the uniform contrast observed along individual wires under TEM (Fig. 5B) indicate the uniformity of *t*-Se nanowire templates was maintained during this chemical transformation. The electron diffraction pattern (see inset) obtained from an individual nanowire suggests these as-synthesized nanowires of Ag_2Se were single-crystalline. This pattern was also in agreement with a tetragonal structure, with the longitudinal axis oriented along the <001> direction. The high resolution TEM image, shown in Figure 5C, further supports the claim of single-crystallinity for the Ag_2Se nanowires synthesized using the present procedure. The 0.25 nm spacing of the fringes calculated from this image agreed well with the expected separation between the (002) lattice planes. It has been previously proposed that the low-temperature form of Ag_2Se could, in fact, possess two different polymorphic forms depending on the sizes of the single-crystalline domains.[25] A conclusive statement on this issue has been elusive because the polycrystalline films used in these studies were characterized by domains sizes spreading across a very broad range. To our knowledge, the nanowire system described here represents the first example of 1D nanostructures exhibiting a diameter-dependent crystal structure.

2.5. Topotactic Transformation as a Plausible Mechanism

Although the exact mechanism responsible for this crystal-to-crystal transformation is not completely understood at this point, a plausible one is illustrated in Figure 6. We believe a minimal reorganization of structure in the parent solid was the

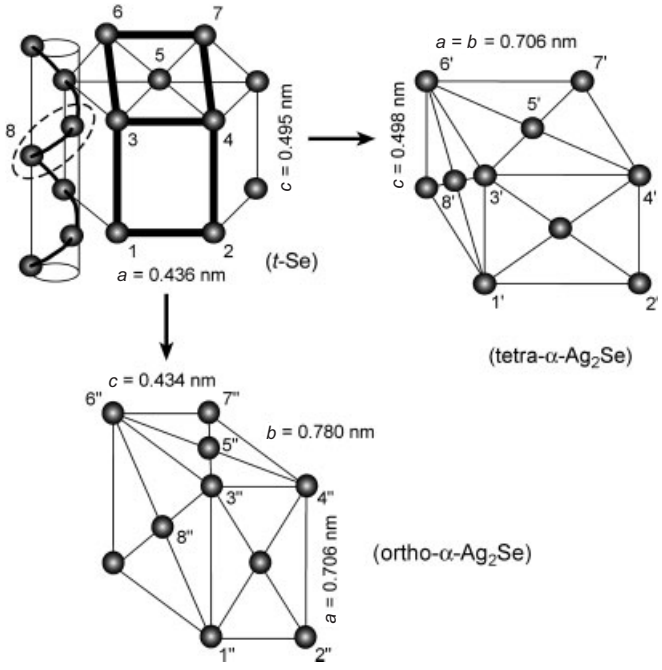

Fig. 6. Illustration of a plausible mechanism for the formation of single-crystalline α-Ag_2Se nanowires from single-crystalline templates—nanowires of *t*-Se. Note that the lattice constant of the *c*-axis for *t*-Se was maintained for the formation of tetragonal α-Ag_2Se; and the lattice constant of the *a*-axis was retained for the formation of orthorhombic α-Ag_2Se. Only selenium atoms or ions were shown in these drawings. In this proposed mechanism, the basic template structure was the lattice formed by selenium atoms 1–7 (indicated by thick lines in the hexagonal lattice of *t*-Se). One of the two #8 selenium atoms (circled) was removed from the *t*-Se lattice, and the other one was shifted to the position of #8′ or #8″ in the templating process. As illustrated, the basic structure was unchanged topologically in one of the three dimensions when α-Ag_2Se was formed.

  1616-301X/02/1010-0683 $ 17.50+.50/0

key to the formation of single-crystalline products from single-crystalline templates. When silver ions diffused into the single-crystalline nanowires of *t*-Se,[26] the silver ions might catalyze a disproportional process of Se^0 into Se^{2-} and Se^{4+}. The Se^{4+} species diffused out of the solid matrix and reacted with Ag^+ and H_2O to generate Ag_2SeO_3 in the aqueous medium around the templates. The Se^{2-} species combined with the trapped Ag^+ cations to generate single-crystalline nanowires of α-Ag_2Se. On another account, the Ag^+ cations could be reduced to Ag atoms when they diffused into the *t*-Se template, and subsequent reaction between Ag and Se atoms led to the formation of Ag_2Se within the solid matrix of each individual nanowire:

$$6Ag^+_{(aq)} + Se_{(s)} + 3H_2O \rightarrow 4Ag + Ag_2SeO_{3(s)} + 6H^+_{(aq)} \quad (3)$$

$$4Ag + 2Se \rightarrow 2Ag_2Se_{(s)} \quad (4)$$

No matter which one of the above two paths the reaction followed, the lattice constant in the *c*- or *a*-axis of *t*-Se was essentially unchanged during the formation of tetragonal or orthorhombic α-Ag_2Se, respectively. In particular, a change in the fringe spacing from 0.16 nm to 0.25 nm (see the HRTEM images in Figures 1C and 5C) suggested that only one layer of selenium atoms (perpendicular to the *c*-axis) needed to be removed from each primitive lattice when the tetragonal α-Ag_2Se solid was formed. As a result, the positions and arrangements of Se atoms in the solid template should remain largely unaffected during the course of this reaction. The topotactic characteristics of this process resemble many intercalation reactions that are well documented for their minimal structural reorganization.[27] We believe it was this topotactic feature that had led to the formation of single-crystalline products by templating against single-crystalline nanowires. As for the dependence of Ag_2Se structure on the wire diameter, it seems to be that the nanowires preferentially chose to expand along the longitudinal axis and thus to form the tetragonal structure when the diameter was relatively large (> 40 nm). When the diameter of nanowires was reduced to the range below 40 nm, the nanowire preferentially chose to expanded in the lateral dimensions and ended up in the orthorhombic structure.

2.6. Templating Against Silver Nanowires

We also studied a complementary system in which silver (rather than selenium) nanowires were used as the chemical template. In this case, bi-crystalline silver nanowires of ~100 nm in diameter were first synthesized using the solution-phase procedure described in a communication from our group.[28] Orthorhombic Ag_2Se was formed in a following step by reacting these silver nanowires with a dispersion (in ethanol) that contained colloidal particles of Se. Different from the transformation that involved the use of *t*-Se nanowires as the templates, the reaction between silver nanowires and Se colloids took more than 30 days to completely transform Ag nanowires into Ag_2Se. Figure 7 shows the XRD patterns for this reaction taken at various stages over the course of ~30 days.

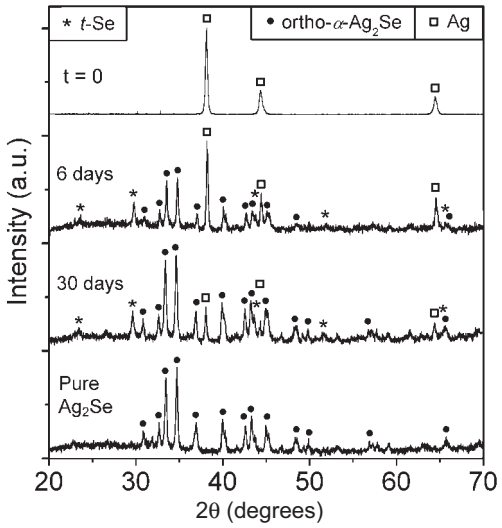

Fig. 7. The XRD patterns of ~100 nm silver nanowires after being mixed with dispersions of selenium colloids in ethanol for designated lengths of time (offset for clarity). All the peaks could be indexed to those of cubic silver, trigonal selenium, or orthorhombic silver selenide. These patterns indicated that bi-crystalline nanowires of silver could be converted to silver selenide by reacting the selenium colloid dispersions for 30 days while stored in dark at room temperature. The pattern for pure orthorhombic silver selenide nanowires (obtained from the reaction between selenium nanowire and silver nitrate solutions) is included for comparison.

Assignment of the peaks clearly indicates the partial conversion of pure metallic silver to a mixture of orthorhombic Ag_2Se and metallic silver after this reaction had been allowed to proceed for ~6 days. The characteristic peaks for silver decreased further over the course of time as the peaks for silver selenide greatly increased in intensity. After ~30 days, the conversion was nearly completed with only a small amount of silver still present in the reaction mixture. The slowness of this transformation process (relative to the reaction that used *t*-Se nanowires as the template) may be attributed to the low solubility of Se colloids in ethanol. It might also be related to the slow diffusion of silver atoms through a solid matrix. Although recent TEM studies indicated that silver atoms could be highly mobile at RT,[29] they should diffuse at a relatively slower rate in a solid matrix than silver ions do. Silver ions have been the major component of many superionic conductors (such as AgI and Ag_2Se) as a result of their extremely small diffusion barriers (or activation energies) at RT.[30]

The morphology of Ag_2Se nanostructures obtained through this templating reaction was also different from that formed by reacting Se nanowires with $AgNO_3$ solutions. Figure 8 gives TEM images of silver nanowires before and after reacting with Se colloids, clearly showing the morphological change involved in this process. The electron diffraction pattern (inset of Fig. 8A) obtained by focusing the electron beam on an individual nanowire suggests a bi-crystalline structure for these nanowires. This diffraction pattern also maintained the same orientation along the longitudinal axis of each nanowire. The Ag_2Se nanostructures resulted from this reaction were polycrystalline, with a characteristic tubular morphology (as shown in Fig. 8B). In this case, the Ag_2Se seemed to be formed around each silver template when the silver atoms were brought into contact with

  1616-301X/02/1010-0684 $ 17.50+.50/0

ADVANCED FUNCTIONAL MATERIALS

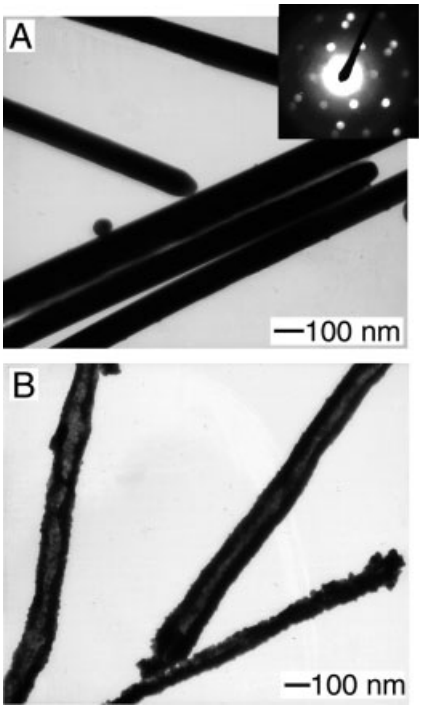

Fig. 8. A) TEM image of silver nanowires synthesized using a solution-phase approach. The inset gives a microdiffraction pattern obtained by focusing the electron beam on an individual nanowire. As determined from the diffraction pattern, these nanowires were bi-crystalline with a (111) twin plane. B) A TEM image of the polycrystalline nanotubes of α-Ag_2Se obtained by reacting the silver nanowires with a dispersion containing *a*-Se colloids. Assignment of the phase was confirmed by both X-ray and electron diffraction analysis.

the selenium source at the interface. The silver atoms had to penetrate (or diffuse through) the barrier of product in order to continuously react the Se atoms. This might explain why the templating reaction between Ag wires and Se colloids was much slower than those based on the reaction between *t*-Se templates and Ag^+ cations.

Although the products were always Ag_2Se for both templating processes described above, they could be remarkably different in morphology and crystallinity depending on the choice of solid templates: single-crystalline Ag_2Se nanowires were formed from selenium templates while polycrystalline Ag_2Se nanotubes were formed from silver templates. These differences represent a manifestation of the different mechanisms involved in each templating process. For the selenium nanowire templates, the silver ions were introduced outside of the nanowires and diffuse inward through the entire templates. The selenium ions do not have to move as much and the single-crystallinity of each template is essentially preserved. Conversely, when amorphous selenium is added to the silver nanowire templates, it is the template material itself, which migrates. As the selenium colloids come into contact with the template nanowires, the silver is oxidized, and the resultant ions migrate outward to form silver selenide solid. This outward migration will lead to the formation of tubular nanostructures characterized by hollow interiors of the same dimensions as the original templates. Silver selenide, in this case, nucleates simultaneously at the multiple contact points (with the selenium colloids) along the longitudinal axis of each silver nanowire. As a result, the Ag_2Se nanostructures are polycrystalline. Since anions generally occupy most of the spaces of an inorganic solid, we can design systems where the anions of the product will come directly from the template (rather than from the gaseous or liquid reagents) in an effort to obtain single-crystalline products.

3. Conclusions

We have demonstrated an effective route for the conversion of one nanostructured material to another. The transformation of selenium to silver selenide may be unique in that the high mobility of silver ions allows the formation of single-crystalline products at RT. We believe this synthetic strategy should be extendable to other systems. For example, selenium is also reactive toward a wealth of other chemicals, and all these chemical reactions can be potentially exploited to convert selenium into other functional materials such as Bi_2Se_3, ZnSe, and CdSe.[32] The activation of cation diffusion through heating might be needed in some cases. The major requirement for the formation of single-crystalline (versus polycrystalline) products will be to keep reconstruction of the template crystal lattice to a minimum. As we have demonstrated here, this requirement could be easily met by designing a reaction system where the anions were provided by the templates while the metal cations were supplied through the gaseous or solution-phase reactant(s). Since the present templating process can be effectively carried out at ambient temperature and pressure, it should be straightforward to scale it up for high-volume production of 1D functional nanostructures. Another major advantage of this templating process is that the templates are consumed during the reaction, leaving the products generally as pure solids free of contaminants. In comparison, products obtained through methods based on physical templates often contain surfactants, block copolymers, or the skeleton of a porous membrane from which the 1D nanostructures have to be isolated after the synthesis.

4. Experimental

Chemicals and Materials: Selenious acid (H_2SeO_3, 99.999 %), silver nitrate ($AgNO_3$, > 99 %), and hydrazine (N_2H_4, 98 %) were purchased from Aldrich (Milwaukee, WI). All chemicals were used as received without further purification. Reaction solutions were prepared by dissolving appropriate amounts of the materials in 18 MΩ water (E-Pure, Dubuque, IA). Polished silicon (100) wafers (test grade, phosphorus-doped) were obtained from Silicon Sense (Nashua, NH). Pre-cleaned glass slides (Micro slides #2947) were purchased from Corning Glass (Corning, NY). Copper and gold grids (coated with amorphous carbon) for TEM studies were obtained from Ted Pella (Redding, CA). All reaction vessels and glassware were pre-cleaned with 18 MΩ water.

Reaction Procedure: Selenium nanowires supported on TEM grids (or as aqueous suspensions) were allowed to react for > 15 h (while stored at ~22 °C in the dark) with aqueous solutions of silver nitrate [30]. Similar morphologies and structural changes were observed for both dispersed and supported nanowires when reacting at the same Se/Ag^+ mole ratio. Reactions were carried out for a set of Se/Ag^+ molar ratios in the range of 1:1 to 1:50, and the completeness of reaction was monitored as a function of the reaction time and the concentration of silver nitrate. For reactions with *t*-Se nanowires (< 0.001 nmol) supported on TEM grids, 1 mL of metal ion solutions with concentrations from 0.3 to 13 nM were used. For reactions with aqueous suspensions of *t*-Se nanowires (~ 76 mM),

  1616-301X/02/1010-0685 $ 17.50+.50/0

1 mL of *t*-Se solution was reacted with an equal volume of metal ion solution ranging from 76 mM to 3.8 M. Products were dried in vacuum and rinsed with hot water (~90 °C) to remove ortho-α-Ag_2Se. Typical yields of single-crystalline Ag_2Se were on the order of 60–70 %.

For the reactions between silver nanowires and selenium colloids, the Se:Ag molar ratios were typically between 1:1 and 1:3. The silver nanowires were prepared as a ~100 mM dispersions in ethanol. 1 mL of the silver dispersion was then mixed with an equal volume of selenium colloid dispersion (~100 mM or ~300 mM). They were allowed to react in the dark and at RT for a period of 30 days. Recoverable yields of polycrystalline Ag_2Se (after rinsing with hot water) were on the order of 20–30 %.

Instrumentation: SEM images were obtained using a field emission microscope (FSEM, JEOL-6300F, Peabody, MA) or an environmental microscope (ESEM, Electroscan-2020, Wilmington, MA). The FSEM was operated with an accelerating voltage of 15 kV, and the ESEM was operated with an accelerating voltage of 20–30 kV and a chamber pressure of ~5 torr. For SEM, all samples were prepared by placing small drops of the nanowire suspensions on silicon substrates, and allowing the solvent to evaporate slowly at RT. The TEM samples were prepared by spotting small drops of diluted (by ~20 times) nanowire solutions on the grids, and followed by slow evaporation of solvent at RT. The TEM images and electron diffraction patterns were taken with a JEOL-1200EX II microscope operated at 80 kV. The electron diffraction patterns were recorded via convergent-beam microdiffraction on individual nanowires (with a beam size of ~100 nm), or selected-area-electron-diffraction (SAED) that involved a random assembly of nanowires. All SEM and TEM samples were not rinsed with water (or any other solvent) before imaging. High-resolution TEM images and EDX spectra were obtained using a Philips CM200 (200 kV) at the Electron Microscopy Facility of Lawrence Berkeley Laboratories (Berkeley, CA). X-ray diffraction (XRD) measurements were obtained on a Philips PW1710 diffractometer using Cu Kα radiation ($\lambda = 0.15418$ nm). The samples for XRD were supported on glass substrates.

Received: April 13, 2002
Final version: May 19, 2002

[1] a) Z. L. Wang, *Adv. Mater.* **2000**, *12*, 1295. b) C. Dekker, *Phys. Today* **1999**, *52*, 22. c) S. Frank, P. Poncharal, Z. L. Wang, W. A. de Heer, *Science* **1998**, *280*, 1744. d) S. J. Tans, M. H. Devoret, H. Dal, A. Thess, R. E. Smalley, L. J. Gerrligs, C. Decker, *Nature* **1997**, *386*, 474. e) M. Bockrath, D. H. Cobden, P. L. McEuen, N. G. Chopra, A. Zettl, A. Thess, R. E. Smalley, *Science* **1997**, *275*, 1922. f) R. Martel, T. Schmidt, H. R. Shea, T. Hertel, P. Avouris, *Appl. Phys. Lett.* **1998**, *73*, 2447.

[2] a) X. Duan, Y. Huang, Y. Cui, J. Wang, C. M. Lieber, *Nature* **2001**, *409*, 66. b) H. M. Huang, S. Mao, H. Feick, H. Yan, Y. Wu, H. Kind, E. Weber, R. Russo, P. Yang, *Science* **2001**, *292*, 1897.

[3] a) J. Hu, T. W. Odom, C. M. Lieber, *Acc. Chem. Res.* **1999**, *32*, 435. b) S. M. Prokes, K. L. Wang, *MRS Bull.* **1999**, *24(8),* 13.

[4] a) G. A. Ozin, *Adv. Mater.* **1992**, *4*, 612. b) H. Weller, *Angew. Chem.*, *Int. Ed. Engl.* **1993**, *32*, 41. c) J. H. Fendler, *Chem. Rev.* **1987**, *87*, 877. d) Y. Xia, J. A. Rogers, K. Paul, G. M. Whitesides, *Chem. Rev.* **1999**, *99*, 1823.

[5] a) N. G. Chopra, R. J. Luyken, K. Cherrey, V. H. Crespi, M. L. Cohen, S. G. Louie, A. Zettl, *Science* **1995**, *269*, 966. b) J. Kong, H. T. Soh, A. M. Cassell, C. F. Quate, H. Dai, *Nature* **1998**, *385*, 878.

[6] a) Z. W. Pan, Z. R. Dai, Z. L. Wang, *Science* **2001**, *291*, 1947. b) S. T. Lee, N. Wang, Y. F. Zhang, Y. H. Tang, *MRS Bull.* **1999**, *24(8)*, 36. c) Y. Y. Wu, P. D. Yang, *Chem. Mater.* **2000**, *12*, 605. d) W. Shi, Y. Zheng, N. Wang, C.-S. Lee, S.-T. Lee, *Adv. Mater.* **2001**, *13*, 591. e) T. J. Trentler, K. M. Hickman, S. C. Goel, A. M. Viano, P. C. Gibbons, W. E. Buhro, *Science* **1995**, *270*, 1971.

[7] a) E. I. Givargizov, in *Highly Anisotropic Crystals* (Eds: I. Sunagawa. D. Reidel), Publishing Company, Boston, MA **1987**. b) N. Ozaki, Y. Ohno, S. Takeda, *Appl. Phys. Lett.* **1998**, *73*, 3700. c) M. Yazawa, M. Koguchi, A. Muto, K. Hiruma, *Adv. Mater.* **1993**, *5*, 577. d) R. S. Wagner, W. C. Ellis, *Appl. Phys. Lett.* **1964**, *4*, 89.

[8] a) C. R. Martin, *Science* **1994**, *266*, 1961. b) B. R. Martin, D. L. Dermody, B. D. Reiss, M. Fang, L. A. Lyon, M. J. Natan, T. E. Mallouk, *Adv. Mater.* **1999**, *11*, 1021. c) Z. Zhang, D. Gekhtman, M. S. Dresselhaus, J. Y. Ying, *Chem. Mater.* **1999**, *11*, 1659.

[9] a) Y. J. Han, J. Kim, G. D. Stucky, *Chem. Mater.* **2000**, *12*, 2068. b) M. Huang, A. Choudrey, P. Yang, *Chem. Commun*. **2000**, *12*, 1603. c) C. P. Mehnert, D. W. Weaver, J. Y. Yin, *J. Am. Chem. Soc.* **1998**, *120*, 12 289. d) K. Moller, T. Bein, *Chem. Mater.* **1998**, *10*, 2950.

[10] a) J. M. Schnur, *Science* **1993**, *262*, 1669. b) K. S. Mayya, D. I. Gittins, A. M. Dibaj, F. Caruso, *Nano Lett.* **2001**, *1*, 727.

[11] a) H. Dai, E. W. Wong, Y. Z. Lu, S. Fan, C. M. Lieber, *Nature* **1995**, *375*, 769. b) J. H. Song, B. Messer, Y. Wu, H. Kind, P. Yang, *J. Am. Chem. Soc.* **2001**, *123,* 9714.

[12] W. Han, S. Fan, Q. Li, Y. Hu, *Science* **1997**, *277*, 1287.

[13] B. Gates, Y. Wu, Y. Yin, P. Yang, Y. Xia, *J. Am. Chem. Soc.* **2001**, *123*, 11 500.

[14] M. Kobayashi, *Solid State Ionics* **1990**, *39*, 121.

[15] M. Ferhat, J. Nagao, *Appl. Phys. Lett.* **2000**, *88*, 813.

[16] R. Xu, A. Husmann, T. F. Rosenbaum, M. L. Saboungi, J. E. Enderby, P. B. Littlewood, *Nature* **1997**, *390*, 57.

[17] G. Sáfrán, O. Geszti, G. Radnóczi, P. B. Barna, *Thin Solid Films* **1998**, *317*, 72.

[18] H. Su, Y. Xie, B. Li, Y. Qian, *Mater. Res. Bull.* **2000**, *35*, 465.

[19] W. Wang, Y. Geng, Y Qian, M. Ji, Y. Xie, *Mater. Res. Bull.* **1999**, *34*, 877.

[20] G. Henshaw, I. P. Parkin, G. A. Shaw, *J. Chem. Soc. Dalton Trans.* **1997**, 231.

[21] a) B. Gates, Y. Yin, Y. Xia, *J. Am. Chem. Soc.* **2000**, *122*, 12 582. b) B. Gates, B. Mayers, B. Cattle, Y. Xia, *Adv. Funct. Mater.* **2001**, *12*, 219.

[22] a) D. M. Chizhikov, V. P. Shchastlivyi, *Selenium and Selenides*; Collets Publishing, London **1968**. b) *Selenium* (Eds: R. A. Zingaro, W. C. Cooper), Van Nostrand Reinhold Company, New York **1974**, p. 177.

[23] a) Z. G. Pinsker, C. Ching-liang, R. M. Imamov, E. L. Lapidus, *Sov. Phys. Cryst.* **1965**, *10*, 225. b) T. Sakuma, K Iida, K. Honma, H. Okazaki, *J. Phys. Soc. Jpn.* **1977**, *43*, 538.

[24] Natl. Bur. of Stand. (U.S.), Circ. 539 554, **1955**; Powder diffraction file No. 06-0362.

[25] J. R. Gunter, P. Keusch, *Ultramicroscopy* **1993**, *49*, 293.

[26] *Solid State Chemistry and its Applications* (Ed: A. West), John Wiley & Sons Ltd., Singapore **1989**, p. 417.

[27] C. N. R. Rao, J. Gopalakrishnan, *New Directions in Solid State Chemistry,* Cambridge University Press, Cambridge **1997**, p. 482.

[28] Y. Sun, B. Gates, B. Mayers, Y. Xia, *Nano Lett.* **2002**, *2*, 165.

[29] Silver atoms were highly mobile at room temperature as suggested by an in situ TEM study: M. Giersig, T. Ung, L. M. Liz-Marzan, P. Mulvaney, *Adv. Mater.* **1997**, *9*, 570.

[30] At high molar ratios, the TEM grids made of copper underwent a redox reaction with silver nitrate producing silver nanoparticles at the edges of the grids. All TEM images reported in this work were of nanowires centered within the TEM grids. Identical transformations of the selenium nanowires were observed in a comparative study between gold and copper TEM grids.

  1616-301X/02/1010-0686 $ 17.50+.50/0